Promoting information diffusion through interlayer recovery processes in multiplex networks

Xin Wang,[1] Weihua Li,[1] Longzhao Liu,[1] Sen Pei,[2] Shaoting Tang,[1,*] and Zhiming Zheng[1,†]

[1]*LMIB, BDBC and School of Mathematics and Systems Science, Beihang University, Beijing 100191, China*
[2]*Department of Environmental Health Sciences, Mailman School of Public Health, Columbia University, New York 10032, USA*

For information diffusion in multiplex networks, the effect of interlayer contagion on spreading dynamics has been explored in different settings. Nevertheless, the impact of interlayer recovery processes, i.e., the transition of nodes to stiflers in all layers after they become stiflers in any layer, still remains unclear. In this paper, we propose a modified ignorant-spreader-stifler model of rumor spreading equipped with an interlayer recovery mechanism. We find that the information diffusion can be effectively promoted for a range of interlayer recovery rates. By combining the mean-field approximation and the Markov chain approach, we derive the evolution equations of the diffusion process in two-layer homogeneous multiplex networks. The optimal interlayer recovery rate that achieves the maximal enhancement can be calculated by solving the equations numerically. In addition, we find that the promoting effect on a certain layer can be strengthened if information spreads more extensively within the counterpart layer. When applying the model to two-layer scale-free multiplex networks, with or without degree correlation, similar promoting effect is also observed in simulations. Our work indicates that the interlayer recovery process is beneficial to information diffusion in multiplex networks, which may have implications for designing efficient spreading strategies.

I. INTRODUCTION

The dynamical processes of information diffusion in social networks have been extensively studied for a long time [1–11]. Due to the rapid evolution of different types of online social networks, the means of information diffusion have been greatly changed in recent years. For example, users often own accounts on different online social networks simultaneously, e.g., Twitter, Facebook, Snapchat, Instagram, and LiveJournal. People frequently receive and diffuse knowledge, ideas, or rumors not only in one platform, but also from one online social network to another. Thus the multiplex network approach in which each layer corresponding to a certain online social network is a natural way to describe this information diffusion process [12–16]. In particular, understanding how the interactions between layers affect the ultimate information diffusion outcome is of great importance in both physics and social psychology [6,17–19].

The research of contagion processes in multilayer networks has been gaining much attention recently [20–23]. Many studies focus on how the interconnections or interactions between layers affect the contagion threshold of epidemics [24–26]. Dickison *et al.* applied the susceptible-infected-recovered model to two different interconnected network systems that are either strongly coupled or weakly coupled, and found that the presence of interconnections could enhance epidemic spreading [27]. Buono *et al.* studied the epidemic propagation processes in a partially overlapped multiplex network and suggested that the epidemic threshold of the multiplex network depended on both the topology of each layer and the overlapping fraction [28]. Using a microscopic Markov chain approach, Granell *et al.* showed that the awareness diffusion was able to control the onset of epidemic outbreaks [29].

Moreover, several studies use classical epidemic models to examine information diffusion in multiplex networks [30–33]. These works mainly concentrate on the interlayer contagion mechanism that can significantly affect the scope of information delivery and the critical properties of diffusion processes. In particular, Cozzo *et al.* studied the susceptible-infected-susceptible model on complex networks using a contact-based information-spreading mechanism with interlayer infections, and found that the critical point of the multiplex system was determined by one of the layers [34]. Li *et al.* studied the susceptible-infected-recovered model with an interlayer transmission rate and suggested that the contagion process between layers could greatly enhance the information diffusion [12].

Despite this progress, we still lack a proper understanding of the interlayer recovery processes in information diffusion. In information diffusion, once an individual becomes a stifler in any one of the social networks, he or she should have a probability to become a stifler in all the other social networks immediately, as he or she has already known the rumor and will no longer spread it. This interaction of recovery across layers exhibits a fundamental difference between information diffusion and epidemic spreading. Therefore, it is of particular interest to examine how the interlayer recovery process affects the scope of information delivery, especially the fraction of stiflers on each layer.

In this paper, we present a framework of information diffusion in multiplex networks in which a modified ignorant-spreader-stifler (SIR) model is used to describe rumor spreading within each layer. Here stifler originates from the classical rumor spreading model proposed by Daley and Kendall [35]. It represented the set of individuals who are reluctant to tell stale news and will no longer spread the rumor. Therefore we denote stiflers by R for reluctant, which also corresponds to recovered status in epidemic SIR model. To characterize the interactions between layers, we propose two independent parameters, i.e., the interlayer contagion

---
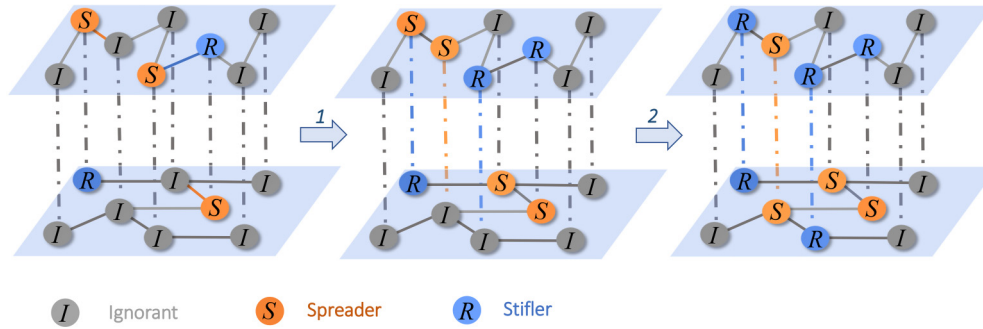*tangshaoting@buaa.edu.cn
†zzheng@pku.edu.cn

FIG. 1. Information diffusion processes on multiplex networks in the modified SIR model with interlayer recovery process. Step 1 refers to the transmission processes within each layer, while step 2 shows both interlayer contagion and recovery processes. The multiplex system will come to a stable state after iterating step 1 and step 2 for a sufficiently long time. Ignorant, spreaders, and stiflers are distinguished with different colors.

rate and the interlayer recovery rate. For multiplex systems composed of two well-mixed populations, two Erdös-Rényi (ER) or scale-free networks, we find that both interlayer recovery and contagion mechanisms can significantly improve the information diffusion processes. In particular, as the interlayer recovery rate increases, the stationary density of stiflers will first increase and then drop gradually, peaking at an optimal rate of interlayer recovery. For homogeneous ER-ER multiplex networks, the optimal interlayer recovery rate can be obtained by solving the evolution equations derived using the mean-field approximation and Markov chain method. The theoretical predictions agree well with simulation results in ER-ER multiplex networks for various parameter settings. Furthermore, we show that the enhancing effect of interlayer recovery mechanism on a certain layer can be improved if information spreads more extensively within the counterpart layer. We also observe similar promoting effects in simulations on two-layer scale-free networks, for both no-degree correlated structure and maximally positive correlated structure (i.e., the node degrees in different layers are maximally correlated in their degree order).

II. MODELING FRAMEWORK

Consider a multiplex system composed of two undirected layers, each standing for an online social platform. Within each layer, N nodes are connected in a network with a given degree distribution. Across layers, the same individual is represented by two counterpart nodes connected by a dashed link as shown in Fig. 1. For simplicity, we assume that there is no degree correlation between layers [36]. The information diffusion first takes place within each layer separately following the SIR rumor diffusion model [37]. In the rumor model, an ignorant (I) represents an agent who has not learned the new information, corresponding to susceptible individuals in epidemiological models. Similarly, spreaders (S) are equivalent to the infected population who can transmit rumors, ideas, or knowledge. Stiflers (R) stand for the people who are aware of the rumor and will no longer spread it, such as the recovered population in epidemic spreading. Complying with the notations in the classical rumor-spreading model, we use $i_k(t) = I_k(t)/N$, $s_k(t) = S_k(t)/N$, and $r_k(t) =$

$R_k(t)/N$ to describe the fraction of ignorant, spreaders, and stiflers in layer k ($k = 1,2$) at time t, respectively, where $i_k(t) + s_k(t) + r_k(t) = 1$. In the classical rumor-spreading SIR model, the recovery process is only caused by the contact interactions with neighbors. However, Wood concluded that the motives from self, others, and reality can change one's attitude and have implications for information processing [38]. This indicates that self is one of the most important origins of attitude change. Therefore taking into account the spontaneous recovery process makes sense. Besides, studies have proven that the information diffusion among social systems can be generated by both peer-to-peer interactions through underlying networks and external social influence from outside of the network [39]. The external social influence, such as the mass media, news web sites, TV, video, books, and so on, plays an important role in the information diffusion process as well [40]. The classical rumor-spreading SIR model only focuses on the peer-to-peer communications via the underlying networks, ignoring the external influence on individuals. However, the spontaneous recovery process can describe the phenomenon that an individual changes his/her status from a spreader to a stifler because of the external social influence to some extent, which will be an effective supplement. To characterize these psychological origins in information diffusion, we assume that two recovery mechanisms coexist in the single-layer SIR process as a modification. One is the spontaneous-recovery transition corresponding to the self-awakening and the other one is the contact-recovery transition, which represents the interaction process of recovery.

We start off by setting a small fraction of nodes as spreaders, while keeping all other nodes ignorant in each layer. The spreaders in two layers are not necessarily the same individuals as the spreaders are chosen independently on each layer. Then the information starts to diffuse within each layer simultaneously according to the following rules. On layer k, a spreader can make its ignorant neighbor become a spreader with a probability λ_k. The spreaders have a probability μ_{k1} to turn into stiflers spontaneously. After that, stiflers can make their neighbor spreaders change to stiflers with a probability μ_{k2}. Here we assume that all the interactions are independent. In the modified SIR model, the likelihood that a spreader becomes a stifler is affected by the states of its neighbors. This

makes it difficult to determine the information transmissibility on a certain link. In this sense, the new SIR process in one single layer is quite different from the classical model used in previous works [41–45]. However, the modified model is more realistic from a psychological perspective, as it accounts for both spontaneous recovery and social contagion processes.

Beyond intralayer transmission, we use θ_1 to characterize how contagion process spreads between layers, i.e., the rate at which an ignorant node gets aware of the information and becomes a spreader if its counterpart on the other layer is a spreader. Additionally, we use θ_2 to denote the probability that an ignorant node or a spreader changes to the stifler state if its counterpart on the other layer is a stifler. To some extent, previous work on interlayer transmission can be regarded as the special case where θ_2 is set to zero. Within this framework, at each time step, information will first spread in each layer independently and then transmit across layers. After a sufficiently long time of evolution, the multiplex system will reach a stationary state, in which the final states are $s_1 = s_2 = 0$, $r_1 = r_2 = r$, and $i_1 = i_2 = i$ if $\theta_2 \neq 0$.

III. THEORETICAL ANALYSIS

A. Intralayer diffusion on well-mixed populations

We first examine how the modified SIR model behaves among well-mixed populations within a single layer and without any network structure as an important limiting case. Under the modified recovery rule, the transmission rate from spreaders to stiflers on layer j ($j = 1,2$) at time t can be written as

$$\mu_j^* = \mu_{j1} + (1 - \mu_{j1})\mu_{j2}r_j(t). \tag{1}$$

The first term accounts for the probability that a spreader becomes a stifler spontaneously, while the second term represents the probability that a spreader recovers under the influence of its neighbors. Therefore, the evolution equations of the densities of ignorants, spreaders, and stiflers within layer j read

$$\frac{di_j}{dt} = -\lambda_j i_j(t)s_j(t), \tag{2}$$

$$\frac{ds_j}{dt} = \lambda_j i_j(t)s_j(t) - \mu_j^* s_j(t), \tag{3}$$

$$\frac{dr_j}{dt} = \mu_j^* s_j(t). \tag{4}$$

The equation for the density of ignorants can be formally integrated, yielding

$$i_j(t) = i_j(0) \exp\left[-\lambda_j \int_0^t s_j(\tau)d\tau\right]. \tag{5}$$

Inserting $r_j(t) = 1 - i_j(t) - s_j(t)$ and Eqs. (2) into Eqs. (4) and neglecting s_j^2 items which is quite small when t becomes larger, we get the following relation valid for a large time t:

$$\int_0^t \frac{dr_j}{dt}dt = (\mu_{j1} + (1 - \mu_{j1})\mu_{j2})\int_0^t s_j(\tau)d\tau$$
$$+ \frac{(1 - \mu_{j1})\mu_{j2}}{\lambda_j}\int_0^t \frac{di_j}{dt}dt, \tag{6}$$

or equivalently

$$\int_0^t s_j(\tau)d\tau = \frac{1}{\mu_{j1} + (1 - \mu_{j1})\mu_{j2}}[r_j(t) - r_j(0)]$$
$$- \frac{(1 - \mu_{j1})\mu_{j2}}{\lambda_j[\mu_{j1} + (1 - \mu_{j1})\mu_{j2}]}[i_j(t) - i_j(0)]. \tag{7}$$

Use $r_j(0) = 0$, $i_j(0) \approx 1$ and $i_{j\infty} + r_{j\infty} = 1$ in Eqs. (5) and let $t \to \infty$. We have

$$i_{j\infty} = e^{-\beta r_{j\infty}}, \tag{8}$$

where $\beta = 1 + \frac{\lambda_j - \mu_{j1}}{\lambda_j[\mu_{j1} + (1 - \mu_{j1})\mu_{j2}]}$. Therefore we finally have the transcendental equation for the fraction of stiflers at the steady state

$$r_{j\infty} = 1 - e^{-\beta r_{j\infty}}. \tag{9}$$

It can also be written as $r_{j\infty} = F(r_{j\infty})$, where $F(x) = 1 - \exp(-\beta x)$ is a monotonously increasing continuous function with $F(0) = 0$ and $F(1) < 1$. Thus a nonzero solution can exist if and only if $F'(0) > 1$, leading to the spreading condition for a finite density of stiflers at large times

$$\lambda_j > \mu_{j1}. \tag{10}$$

Note that among well-mixed populations, the spreading condition is mainly related to the contagion rate and spontaneous recovery rate in our modified SIR model. In addition, we can calculate the final fraction of stiflers precisely by numerically solving Eqs. (2)–(4), or get an approximate solution by solving Eq. (9), which neglects the effects of s_j^2 items.

B. Intralayer and interlayer diffusions on ER-ER multiplex networks

We then consider the case of homogeneous multiplex systems composed of two ER random networks with average degree $\langle k \rangle_1$ and $\langle k \rangle_2$. We will further derive dynamical equations considering both intralayer and interlayer diffusions in this section. We start from the transmission dynamics within each layer. Similar to the last section, the transmission rate from spreaders to stiflers on a single layer can be written using the mean-field approximation as

$$\mu_j^* = \mu_{j1} + (1 - \mu_{j1})[1 - (1 - \mu_{j2})^{\langle k \rangle_j r_j(t)}]. \tag{11}$$

The first term accounts for the spontaneous recovery while the second term represents the effects of the node's neighbors. The evolution equations, which describe the modified SIR processes within a single layer read

$$\frac{di_j}{dt} = -\lambda_j \langle k \rangle_j i_j(t)s_j(t),$$
$$\frac{ds_j}{dt} = \lambda_j \langle k \rangle_j i_j(t)s_j(t) - \mu_j^* s_j(t),$$
$$\frac{dr_j}{dt} = \mu_j^* s_j(t). \tag{12}$$

Now we focus on interactions between layers. For a small value of interlayer contagion rate θ_1, the probability of an individual to be an ignorant or a spreader is approximately independent across layers, since the interlayer contagion only

affects a small number of people [46–48]. Therefore, at time t, the fraction of individuals who are ignorant in layer 1 while at the same time are spreaders in layer 2 can be approximated by $i_1(t)s_2(t)$. This group of individuals contribute to the interlayer contagion process and they can directly change from ignorants to spreaders with the probability θ_1 in layer 1. When dealing with the interlayer recovery process, however, the situation becomes more complicated. The major challenge is that the fraction of population who are ignorants or spreaders in layer 1 and stiflers in layer 2 at time t cannot be naively approximated by $[1 - r_1(t)]r_2(t)$ across all the spreading process. This approximation should be valid at the early stage of the spreading when the number of stiflers in layer 2 is small. However, as the spreading proceeds, stiflers in layer 2 will be accumulated to a relatively large size. Under this condition, in contrast to the interlayer contagion process that involves only a limited number of nodes, the interlayer recovery process can affect a large group of people. Therefore, an individual being a nonstifler in layer 1 and a stifler in layer 2 are far from independent at the later stage of the spreading when stiflers are abundant. An extreme example would be at the steady state of the multiplex system. At this stage, each individual will be either an ignorant or a stifler in both layers. Obviously the fraction of people who are stiflers in layer 2 but still nonstiflers in layer 1 is exactly 0, which cannot be approximated by $(1 - r_1)r_2 \neq 0$.
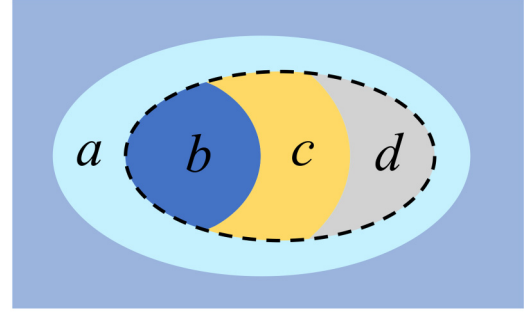
To overcome this difficulty, we use a Markov chain approach. Denote $V_{1i}(T)$ and $V_{1s}(T)$ as the fraction of ignorants and spreaders in layer 1 whose counterparts in layer 2 are stiflers at time T, respectively. We will derive the analytic form of $V_1(T) = V_{1i}(T) + V_{1s}(T)$, which represents the fraction of individuals who are already stiflers in layer 2 but still nonstiflers in layer 1. As shown in Fig. 2, $V_1(T)$ can be calculated recursively by establishing its relation with $V_1(T - 1)$ after a round of evolution between layers and within layer 1. The changes from $V_1(T - 1)$ to $V_1(T)$ are displayed in the Venn diagram in Fig. 2 [49]. Specifically, region a is the increasing part of individuals who have just become stiflers in layer 2 but have not switched to stiflers in layer 1, which can be approximated by $[r_2(T) - r_2(T - 1)][1 - r_1(T)]$. Region b and region c represent the loss of nonstiflers in layer 1 among the population of $V_1(T - 1)$, caused by cross-layer recovery and spontaneous or neighbor influenced recovery respectively. The sizes of these two groups of individuals are $\theta_2 V_1(T - 1)$ and $V_{1s}(T - 1)\mu_1^*$ respectively. Therefore, the remaining population of $V_1(T - 1)$ at time T is simply $(1 - \theta_2)V_1(T - 1) - V_{1s}(T - 1)\mu_1^*$. Summing up both the increasing and remaining population, we get the recursive formula of $V_1(T)$

$$V_1(T) = (1 - \theta_2)V_1(T - 1) - V_{1s}(T - 1)\mu_1^* \\ + [r_2(T) - r_2(T - 1)][1 - r_1(T)], \quad (13)$$

and

$$V_{1s}(T - 1) = V_1(T - 1)\frac{s_1(T - 1)}{i_1(T - 1) + s_1(T - 1)}. \quad (14)$$

The update in layer 2 caused by interlayer contagion and recovery can be obtained in a similar way. We then obtain
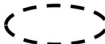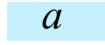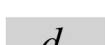

FIG. 2. The Venn diagram for the recursive relation of $V_1(T)$. The dotted oval represents the region of $V_1(T - 1)$. At time T, nodes in region b change to stiflers in layer 1 due to interlayer recovery transitions while nodes in region c also become stiflers following the modified SIR dynamics within layer 1. At the same time, region a represents the increased individuals who have just become stiflers in layer 2 but still not change into stiflers in layer 1. Thus $V_1(T)$ can be calculated by the sum of proportions of region d and region a.

the full evolution equations of the multiplex system

$$i_1(T + 1) = i_1(T) - \lambda_1\langle k\rangle_1 i_1(T)s_1(T) \\ - \theta_1 i_1(T)s_2(T) - \theta_2 V_{1i}(T),$$
$$s_1(T + 1) = s_1(T) + \lambda_1\langle k\rangle_1 i_1(T)s_1(T) - \mu_1^* s_1(T) \\ + \theta_1 i_1(T)s_2(T) - \theta_2 V_{1s}(T),$$
$$r_1(T + 1) = r_1(T) + \mu_1^* s_1(T) + \theta_2 V_1(T),$$
$$i_2(T + 1) = i_2(T) - \lambda_2\langle k\rangle_2 i_2(T)s_2(T) \\ - \theta_1 i_2(T)s_1(T) - \theta_2 V_{2i}(T),$$
$$s_2(T + 1) = s_2(T) + \lambda_2\langle k\rangle_2 i_2(T)s_2(T) - \mu_2^* s_2(T) \\ + \theta_1 i_2(T)s_1(T) - \theta_2 V_{2s}(T),$$
$$r_2(T + 1) = r_2(T) + \mu_2^* s_2(T) + \theta_2 V_2(T) \quad (15)$$

and

$$i_1(t) + s_1(t) + r_1(t) = 1, \\ i_2(t) + s_2(t) + r_2(t) = 1. \quad (16)$$

During the evolution of spreading, it is clear that $V_1(T)$ depends on variables $r_1(t), r_2(t), s_1(t)$, and $i_1(t)$ ($t = 1, 2, \ldots, T - 1$) according to Eqs. (13) and (14). Therefore, it is hard to present the exact analytical form of $V_1(T)$ in terms of these variables. However, our concern is the ultimate state of the multiplex system, i.e., the fraction of stiflers in each layer $r_{j\infty}$ when $t \to \infty$. At the stationary state, we attempt to analytically derive the relationship between $r_{j\infty}$

and parameters. From this perspective, for a small value $\varepsilon > 0$, we define a time point T_c such that the increase of stiflers in both layers $r_j(t+1) - r_j(t) < \varepsilon$ and the fraction of spreaders $s_j(t) < \varepsilon$ ($j = 1,2$) for $t \geqslant T_c$. This is feasible because $dr_j(t)/dt = 0$ and $s_j(t) = 0$ ($j = 1,2$) as $t \to \infty$. Under this condition, T_c can be regarded as the demarcation point of the two spreading stages, after which the stiflers in layer 2 compose of a relatively large proportion such that $V_1(T)$ cannot be approximated by $[1 - r_1(T)]r_2(T)$. Following Eqs. (13) and (14), for $T \to \infty$ we have

$$
V_1(T) = V_1(T_c) \prod_{j=1}^{T-T_c} \left(1 - \theta_2 - \frac{s_1(T-j)\mu_1^*}{i_1(T-j) + s_1(T-j)}\right)
$$
$$
+ \sum_{l=1}^{T-T_c} \left\{ [r_2(T-l+1) - r_2(T-l)] \right.
$$
$$
\times [1 - r_1(T-l+1)] \prod_{j=1}^{l-1}
$$
$$
\left. \times \left(1 - \theta_2 - \frac{s_1(T-j)\mu_1^*}{i_1(T-j) + s_1(T-j)}\right)\right\}, \quad (17)
$$

and specially we define

$$
\prod_{j=1}^{0} \left(1 - \theta_2 - \frac{s_1(T-j)\mu_1^*}{i_1(T-j) + s_1(T-j)}\right) = 1 \quad (18)
$$

to deal with the situation when $l = 1$ in Eq. (17).

Now we attempt to simplify Eq. (17) by neglecting the items of the order up to $O(\varepsilon)$. As defined above, it is clear that $r_2(T-l+1) - r_2(T-l) < \varepsilon$ for all $l \leqslant T - T_c$. Because the term $\prod_{j=1}^{l-1}(1 - \theta_2 - \frac{s_1(T-j)\mu_1^*}{i_1(T-j)+s_1(T-j)})$ decreases exponentially and $[1 - r_1(T-l+1)]$ is bounded below 1, we have

$$
\sum_{l=1}^{T-T_c} \left\{ [r_2(T-l+1) - r_2(T-l)][1 - r_1(T-l+1)] \right.
$$
$$
\left. \times \prod_{j=1}^{l-1} \left(1 - \theta_2 - \frac{s_1(T-j)\mu_1^*}{i_1(T-j) + s_1(T-j)}\right)\right\} \sim O(\varepsilon). \quad (19)
$$

Additionally, we have

$$
\frac{s_1(T-j)\mu_1^*}{i_1(T-j) + s_1(T-j)} \sim O(\varepsilon) \quad (20)
$$

for $j = 1,2,\ldots,T-T_c$, as $s_1(T-j) < \varepsilon$ and $i_1(T-j)$ converges to a positive value $i_{1\infty}$. Applying the deductions (19) and (20) to Eq. (17), $V_1(T)$ can be approximately given by

$$
V_1(T) = V_1(T_c)(1 - \theta_2)^{T-T_c}. \quad (21)
$$

Naturally, we extend (21) to the continuous situation and reach to the approximation formula of $V_1(t)$

$$
V_1(t) = \begin{cases} (1 - r_1(t))r_2(t), & t \leqslant T_c \\ V_1(T_c)(1 - \theta_2)^{t-T_c}, & t > T_c. \end{cases} \quad (22)
$$

When $t \to \infty$, we have

$$
V_1(t) = r_2(T_c)[1 - r_1(T_c)](1 - \theta_2)^{t-T_c}. \quad (23)
$$

The approximations of $V_{1i}(t)$ and $V_{1s}(t)$ are listed as follows

$$
V_{1i}(t) = r_2(T_c)i_1(T_c)(1 - \theta_2)^{t-T_c},
$$
$$
V_{1s}(t) = r_2(T_c)s_1(T_c)(1 - \theta_2)^{t-T_c}. \quad (24)
$$

Here we propose two ways to determine T_c. One is to set a fixed small value $\varepsilon^* > 0$ and find a time critical point when $r_j(t+1)/r_j(t) < 1 + \varepsilon^*$ for both layers. The other one is to fix T_c empirically. We observe in simulation that the multiplex system we use tends to be steady within $300 \sim 500$ steps of evolution. In addition, r increases rapidly in early stage of diffusion and then grows slowly. Thus we can set $T_c = 30 \sim 100$, which is not strict but is efficient.

Therefore $i_j(T_c), s_j(T_c), r_j(T_c)$ in layer j can be calculated numerically by substituting $V_1(t) = [1 - r_1(t)]r_2(t)$ for $t \leqslant T_c$ in Eq. (15). Analysis of layer 2 follows the same way. Finally, substituting $s_j(t), V_j(t), V_{ji}(t)$, and $V_{js}(t)$ ($j = 1,2$) in the continuous form of Eq. (15) by using Eqs. (16), (23), and (24), the nonlinear approximating differential equations for the evolution processes read

$$
\frac{di_1}{dt} = -\lambda_1 \langle k \rangle_1 \, i_1(t)[1 - i_1(t) - r_1(t)]
$$
$$
- \theta_1 i_1(t)[1 - i_2(t) - r_2(t)]
$$
$$
- \theta_2 r_2(T_c) i_1(T_c)(1 - \theta_2)^{t-T_c},
$$
$$
\frac{dr_1}{dt} = \mu_1^*[1 - i_1(t) - r_1(t)]
$$
$$
+ \theta_2 r_2(T_c)[1 - r_1(T_c)](1 - \theta_2)^{t-T_c},
$$
$$
\frac{di_2}{dt} = -\lambda_2 \langle k \rangle_2 \, i_2(t)[1 - i_2(t) - r_2(t)]
$$
$$
- \theta_1 i_2(t)[1 - i_1(t) - r_1(t)]
$$
$$
- \theta_2 r_1(T_c) i_2(T_c)(1 - \theta_2)^{t-T_c},
$$
$$
\frac{dr_2}{dt} = \mu_2^*[1 - i_2(t) - r_2(t)]
$$
$$
+ \theta_2 r_1(T_c)[1 - r_2(T_c)](1 - \theta_2)^{t-T_c}. \quad (25)
$$

IV. RESULTS

A. Theoretical and simulation results on multiplex well-mixed populations

We start from a multiplex system composed of two well-mixed populations. Each layer has $N = 10^3$ nodes. Initially we have ten spreaders in each layer, i.e., $i_j(0) = 0.99$ and $s_j(0) = 0.01$ on layer j, $j = 1,2$.

We show how the modified SIR model behaves in a single layer among well-mixed population in Fig. 3. We set $\theta_1 = \theta_2 = 0$ to exclude the influence of interlayer dynamical processes. In Fig. 3(a), we give three groups of μ_{11}, μ_{12} and present the stationary fraction of stiflers in layer 1 as a function of λ_1. Our theoretical predictions produced by numerically solving differential equations (2)–(4) can well match the simulation results, as shown in Fig. 3(a) by solid lines. The approximate solutions solved by Eqs. (9) are also presented by dash lines. Naturally, the threshold of information diffusion increases as μ_{11} becomes larger, which can also be observed in Eqs. (10). It is worthy of noting that among well-mixed populations where the contagion process is less efficient compared with
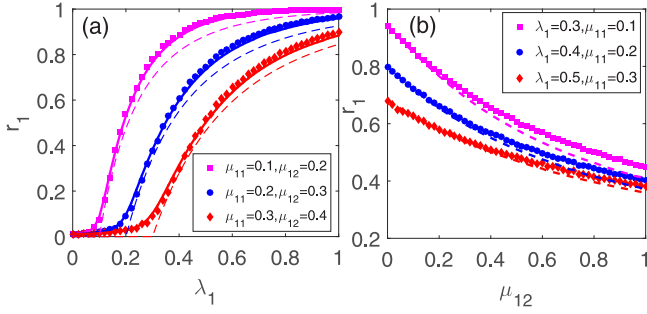
FIG. 3. How modified SIR model behaves in a single layer among well-mixed population. (a) The stationary fraction of stiflers in layer 1 is presented as a function of λ_1. We set $\mu_{11} = 0.1, \mu_{12} = 0.2$; $\mu_{11} = 0.2, \mu_{12} = 0.3$; $\mu_{11} = 0.3, \mu_{12} = 0.4$, respectively. The other parameters are set as follows, $N = 10^3, \theta_1 = \theta_2 = 0$. Theoretical predictions produced by Eqs. (2)–(4) are shown by solid lines, while theoretical solutions solved by Eqs. (9) are shown by dash lines. (b) How contact-recovery mechanism affects the stationary fraction of stiflers. We fix $\lambda_1 = 0.3, \mu_{11} = 0.1$; $\lambda_1 = 0.4, \mu_{11} = 0.2$; $\lambda_1 = 0.5, \mu_{11} = 0.3$, respectively and change μ_{12} from 0 to 1. The other parameters are set as follows, $N = 10^3, \theta_1 = \theta_2 = 0$. Theoretical predictions produced by Eqs. (2)–(4) are shown by dashed lines.

a network-structured population, the fraction of stiflers is less than 1 as μ_{11}, μ_{12} increases even when $\lambda_1 = 1$. In Fig. 3(b), we further explore the effects of contact-recovery mechanism on the stationary fraction of stiflers. We fix λ_1, μ_{11} and change μ_{12} from 0 to 1. Results show that the stationary fraction of stiflers decreases significantly as μ_{12} becomes larger. Our theoretical predictions using Eqs. (2)–(4) agree well with the simulation results when μ_{12} is not too large, as shown in Fig. 3(b). As μ_{12} approaches to 1, we find that λ_1 is much smaller than μ_1^* when the system becomes steady, which means there exists a time period that the recovery rate is always larger than the contagion rate. This leads to minor errors of our predictions.

We also present the effects of interlayer recovery process on the stationary fraction of stiflers among multiplex well-mixed populations in Fig. 4. We give three sets of $\lambda_j, \mu_{j1}, \mu_{j2}$, and set $\theta_1 = 0$ in Figs. 4(a) and 4(c) while we fix the parameters $\lambda_j, \mu_{j1}, \mu_{j2}$ and change $\theta_1 = 0, 0.1, 0.2$, respectively in Figs. 4(b) and 4(d). In this way, we attempt to establish a firm grasp of how the interlayer recovery process, which is directly controlled by the parameter θ_2, affects information diffusion under different circumstances. Results show that the scope of information delivery is effectively promoted by the interlayer recovery process when θ_2 is not too large. Note that in Fig. 4(b), a large θ_2 shows an inhibitive effect on information diffusion when $\theta_1 > 0$. An interesting phenomenon can also be observed that in all cases a small interlayer recovery rate has the maximal promoting effects. Additionally, all peak points, i.e., the turning points of the curves, appear in the vicinity of $\theta_2 = 0.01 \sim 0.02$ in our simulations, according to Figs. 4(c) and 4(d), which show a detailed view of how θ_2 behaves.

We will add network structures and further explore the behaviors of interlayer recovery process in the next two sections. Moreover, theoretical predictions of the peak points will be shown in multiplex systems composed of two ER
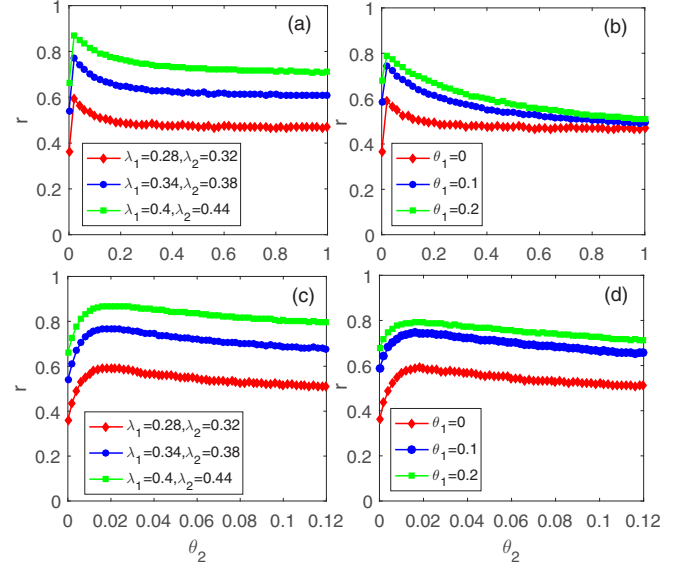

FIG. 4. Effects of the interlayer recovery process on the stationary fraction of stiflers among well-mixed populations. (a) We set $N = 10^3, \theta_1 = 0, \mu_{11} = \mu_{12} = \mu_{21} = \mu_{22} = 0.2$ for the three curves. Other parameters are set as follows: diamond: $\lambda_1 = 0.28, \lambda_2 = 0.32$; circle: $\lambda_1 = 0.34, \lambda_2 = 0.38$; square: $\lambda_1 = 0.4, \lambda_2 = 0.44$. (b) We change $\theta_1 = 0, 0.1, 0.2$ to observe the influence of dynamical processes between layers. Other parameters are fixed: $N = 10^3, \lambda_1 = 0.28, \mu_{11} = \mu_{12} = 0.2, \lambda_2 = 0.32, \mu_{21} = \mu_{22} = 0.2$. (c) and (d) show a detailed view of how θ_2 behaves, corresponding to (a) and (b) respectively.

networks. Explanations for the behaviors of our modified SIR model as well as the influence of interlayer recovery process will also be given.

B. Theoretical and simulation results on two ER networks

We construct a multiplex system composed of two ER networks with $N = 10^4$ nodes in each layer, with no degree correlations between layers. We set $\langle k \rangle_1 = 20$ for layer 1 and $\langle k \rangle_2 = 30$ for layer 2. Initially, we have ten spreaders in each layer, i.e., $i_j(0) = 0.999$ and $s_j(0) = 0.001$. To make the analysis more tractable, we assume $\mu_{j1} = \mu_{j2} = \mu_j (j = 1, 2)$ in Eq. (11) to simplify the dynamical process within the same layer in the following parts. Extensive simulations are implemented to crosscheck our theoretical analysis.

First, the results of modified SIR processes within a single layer are shown in Fig. 5. In this scenario, we simply set $\theta_1 = \theta_2 = 0$, which means the information diffusion processes only occur within each layer separately. The stable fraction of stiflers in layer i simply depends on λ_i and μ_i. Theoretical analyses using Eqs. (12) and simulation results are presented in Fig. 5. Theoretical lines can match the simulation results quite well. It is worth noting that in the classical rumor spreading SIR model, the rumor always has a nonzero probability of pervading a macroscopic fraction of the system whatever the values of the rates λ and μ are [37]. However, our modified SIR process exhibits a continuous phase transition as shown in Fig. 5. This is due to the fact that when r_i is quite small, $\mu_i^* \approx \mu_{i1}$. This implies, the spontaneous recovery process becomes the main channel to recover. Under this circumstance,
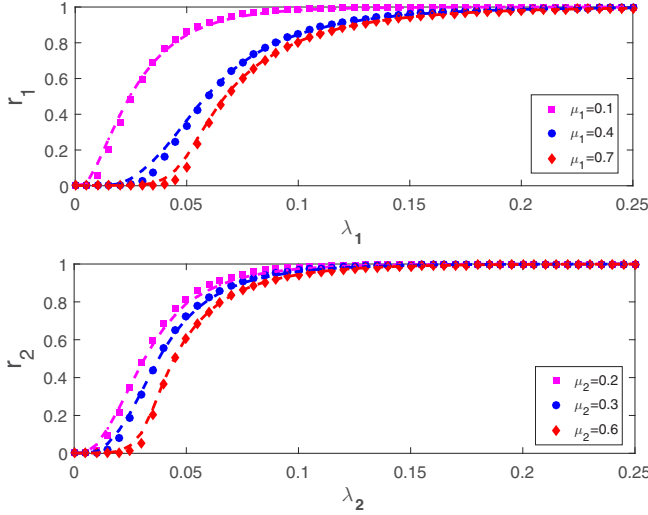
FIG. 5. Information diffusion results within each layer, i.e., the stationary fraction of stiflers in layer $i(i = 1,2)$ as a function of λ_i. The other parameters for the underlying multiplex networks and the dynamical processes are set as follows, $N = 10^4, \langle k \rangle_1 = 20, \langle k \rangle_2 = 30, \theta_1 = \theta_2 = 0$. Theoretical predictions produced by Eqs. (12) are shown by dash lines.

$\frac{dr_i}{dt} \approx \mu_{i1}s_i(t)$, which is similar to the recovery mechanism of classical susceptible-infected-recovered model in disease propagation [37].

We then examine the effect of interlayer contagion process on the stationary fraction of stiflers in each layer. We set $\theta_2 = 0$ to make information contagion processes as the only dynamical interactions between layers. In Fig. 6, we present both theoretical and simulation results for the stable fraction of stiflers in layer i as a function of θ_1. The stifler fraction r_i greatly increases as θ_1 grows. This indicates that the interlayer contagion process can remarkably extend the scale of information diffusion in multiplex systems. This is because the fraction of spreaders in a certain layer can increase significantly due to the interlayer contagion transmission, and spreaders will eventually become stiflers in the steady state.
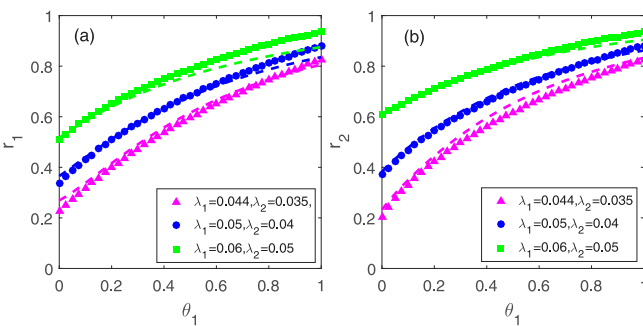

FIG. 6. Effects of the interlayer contagion process on the stationary fraction of stiflers in each layer. Theoretical results produced by Eq. (25) are shown with dashed lines. The parameters are set as $N = 10^4, \langle k \rangle_1 = 20, \langle k \rangle_2 = 30, \theta_2 = 0, \mu_1 = 0.4, \mu_2 = 0.6$. Other parameters in (a) and (b) include: triangle: $\lambda_1 = 0.044, \lambda_2 = 0.035$; circle: $\lambda_1 = 0.05, \lambda_2 = 0.04$; square: $\lambda_1 = 0.06, \lambda_2 = 0.05$.
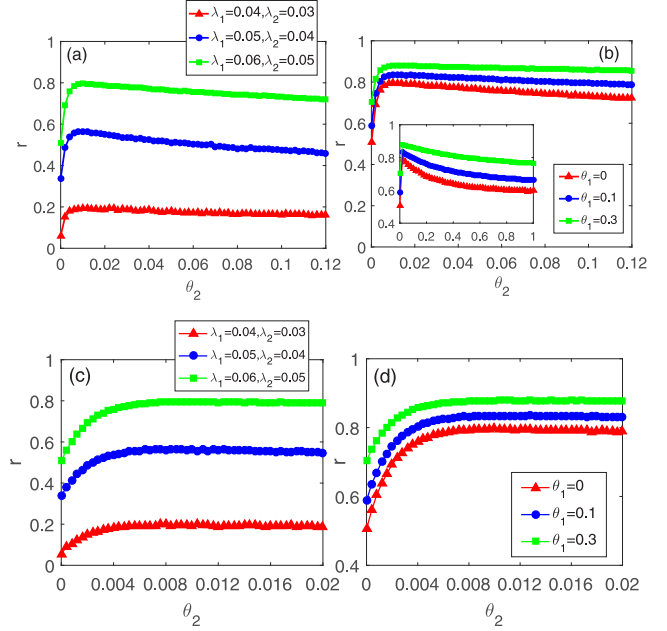

FIG. 7. Effects of the interlayer recovery process on the stationary fraction of stiflers. We present density of stiflers at the steady state as a function of θ_2 for the multiplex system composed of two ER networks with $N = 10^4$ nodes. (a) We set $\theta_1 = 0, \mu_1 = 0.4, \mu_2 = 0.6$ for the three curves. Other parameters are set as follows: triangle: $\lambda_1 = 0.04, \lambda_2 = 0.03$; circle: $\lambda_1 = 0.05, \lambda_2 = 0.04$; square: $\lambda_1 = 0.06, \lambda_2 = 0.05$. (b) We change $\theta_1 = 0, 0.1, 0.3$ and fix other parameters: $\lambda_1 = 0.06, \mu_1 = 0.4, \lambda_2 = 0.05, \mu_2 = 0.6$. Inset shows the global trend of the curves. (c) and (d) show a detailed view of how θ_2 behaves in the region where $\theta_2 \ll 1$, corresponding to (a) and (b), respectively.

We also notice that the theoretical results agree well with the simulations when θ_1 is not too large. As θ_1 approaches to 1, the accuracy of our prediction drops because it is more likely for spreaders to cluster within local areas, which leads to a nonrandom distribution in each layer. In this case, the fraction of individuals who are ignorant in layer k and spreaders in layer j can not be well approximated by $i_k(t)s_j(t)$.

In Fig. 7, we show the impact of interlayer recovery process on information diffusion. In Fig. 7(a), we test three groups of λ_i, μ_i, and set $\theta_1 = 0$. Meanwhile, in Fig. 7(b), the parameters λ_i and μ_i, which control the dynamical processes within each layer are fixed and we change θ_1 to observe the influence of interlayer dynamical processes. To investigate in detail how θ_2 behaves near peaks, we increase the resolution in the region where $\theta_2 \ll 1$ in Figs. 7(c) and 7(d), corresponding to Figs. 7(a) and 7(b) respectively. Each point on the curves is the average of 100 simulations. We denote r as the fraction of stiflers in both layers for $\theta_2 > 0$. According to the evolution rule, it is clear $r = r_1 = r_2$ if $\theta_2 > 0$. For $\theta_2 = 0$, we set r as the smaller one of r_1 and r_2 to observe the effects on the weaker layer where information spreads less broadly. Interestingly, in all circumstances, the fraction of stiflers r increases sharply at first and then decreases gradually as θ_2 becomes larger. However, even when $\theta_2 = 1$, the fraction of stiflers still remains larger than that when there is no interlayer recovery process, i.e., $\theta_2 = 0$. In summary, the interlayer recovery mechanism
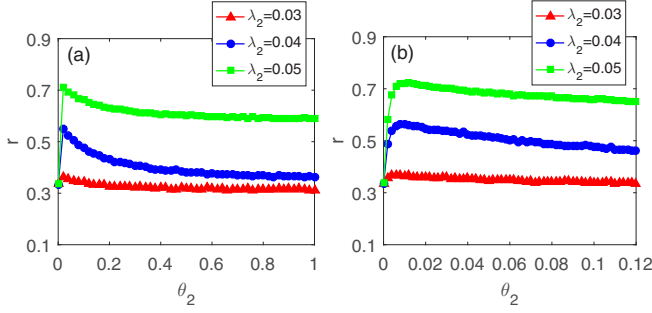
FIG. 8. How dynamical processes within a certain layer affect the promoting effect of interlayer recovery process on the counterpart layer. We set $\lambda_1 = 0.05$, $\mu_1 = 0.4$, $\mu_2 = 0.6$, and $\lambda_2 = 0.03, 0.04, 0.05$, respectively. Here we fix $\theta_1 = 0$ to exclude the influence of contagion process between layers. The global trend of curves is shown in (a) while the results near peaks are displayed in (b).

promotes the information diffusion in multiplex systems. Particularly, the enhancing effect is optimized at a small interlayer recovery rate. As shown in Figs. 7(c) and 7(d), all the average peaks appear in the range of $\theta_2 = 0.006 \sim 0.014$, or in the vicinity of $\theta_2 = 0.01$. The peak points here are of great importance to further develop efficient information diffusion strategies. This phenomenon can be explained by the following reasoning. When θ_2 is small, the interlayer recovery processes help a small fraction of ignorants and spreaders to become stiflers and thus promote the information spreading within each layer. However, when θ_2 becomes large, a larger fraction of ignorants and spreaders directly change into stiflers, which leads to a significant reduction of spreaders within each layer. In other words, some individuals just skip the spreader state and no longer spread the information before the system becomes stable. To some extent, a large θ_2 has an inhibitive effect for information spreading among the whole multiplex system.

In addition, we also discuss how dynamical processes within a certain layer affect the promoting effect of interlayer recovery process on the counterpart layer. In Fig. 8, we analyze diffusion results as a function of λ_2 by fixing λ_1, μ_1, and θ_1, so that we can learn about how changes on layer 2 affect the enhancing effect on layer 1. As shown in simulations, the enhancing effect of interlayer diffusion on layer 1, characterized by θ_2, becomes more significant as λ_2 rises. Thus, the promoting effect of interlayer recovery mechanism on one layer can be strengthened if information spreads more sufficiently on the other layer.

Furthermore, we present both theoretical predictions and simulation results of the optimal interlayer recovery rate θ_2^* that achieves the maximal enhancing effect. In Fig. 9, the distribution of θ_2^* in 100 simulations are shown by box plots, illustrating the 0th, 25th, 50th, 75th, and 100th percentiles. When calculating theoretical predictions by Eq. (25), we choose to fix $T_c = 40, 60, 100$, respectively which is more efficient as mentioned earlier. It can be observed that all optimal rates fluctuate near 0.01, but the relative fluctuations is large in different simulations. Most of the theoretical results fall within the range of simulated values. Note that the absolute
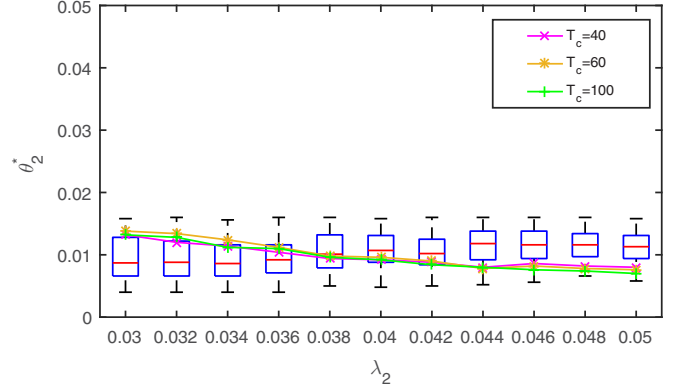

FIG. 9. Theoretical predictions and simulation results of the optimal interlayer recovery rate that achieves the maximal enhancing effect. We use box plots to show the distribution of peak positions in 100 independent simulations. From bottom to top, the box shows the 0th, 25th, 50th, 75th, and 100th percentiles. We change $T_c = 40, 60$, and 100 respectively in Eqs. (25). Other parameters are set as follows: $\lambda_1 = 0.05$, $\mu_1 = 0.4$, $\mu_2 = 0.6$, $\theta_1 = 0$.

error is quite small comparing with the whole parameter range $\theta_2 \in [0,1]$.

C. Simulation results on two scale-free networks

We also apply our model to multiplex systems composed of two scale-free networks. In fact, the underlying structure of real online social networks is closer to scale-free networks in which the preferential attachment mechanism leads to a power-law degree distribution $p_k \propto k^{-\gamma}$ [37]. Studies have shown that the hubs who connect a large number of nodes in scale-free networks can significantly accelerate the transmission processes [50]. Also, we attempt to show how interlayer dynamical processes affect the information diffusion under this two scale-free multiplex networks topology. We generate the scale-free networks using a preferential attachment model, in which the preferential attachment mechanism is given by $p_i \sim k_i + \alpha$. Here k_i is the degree of node i and α denotes the attractiveness of the vertices with no adjacent edges. We add one vertex in each time step and the new vertex initiates m edges to old vertices. Under this circumstance, the exponential value of the scale-free graph can be calculated by $\gamma = 3 + \alpha/m$. We fix $\alpha = 1$ and let $m = 5,7$, respectively. Therefore, we have $\gamma_1 = 3.2$ for layer 1 and $\gamma_2 = 3.14$ for layer 2. In addition, the average degrees of the scale-free networks are 10 and 14, i.e., $\langle k \rangle = 2m$. In our simulations, both layers have 10^4 nodes and we set $s_j(0) = 0.001$.

In Fig. 10 we show the relation between interlayer recovery and contagion process. We present the stationary density of stiflers in layer 1 as a function of interlayer contagion rate. The contagion process between layers can significantly promote the information diffusion processes. We also set two groups of parameters in which $\theta_2 \neq 0$ for comparison. Results show that when θ_1 is small, θ_2 plays a major role in the promoting effects. However, as θ_1 gradually approaches to 1, the effect of θ_2 becomes weaker and θ_1 takes over the major promoting effect. In other words, both interlayer contagion and recovery mechanisms promote the information diffusion processes. The
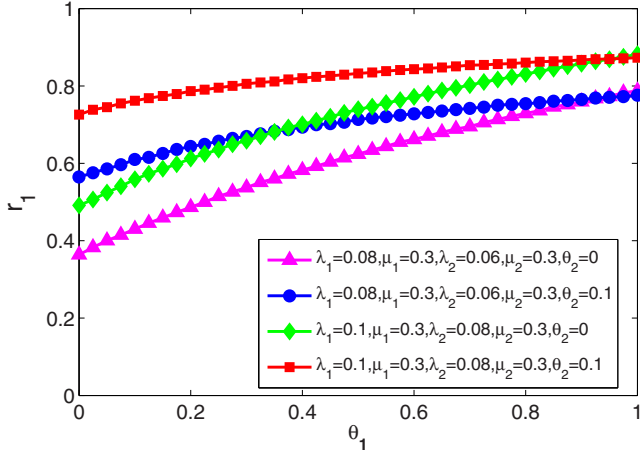
FIG. 10. Simulation results of the stationary fraction of stiflers as a function of contagion rate between layers for a multiplex system composed of two scale-free networks. Other parameters are set as follows: triangle: $\lambda_1 = 0.08$, $\mu_1 = 0.3$, $\lambda_2 = 0.06$, $\mu_2 = 0.3$, $\theta_2 = 0$; circle: $\lambda_1 = 0.08$, $\mu_1 = 0.3$, $\lambda_2 = 0.06$, $\mu_2 = 0.3$, $\theta_2 = 0.1$; diamond: $\lambda_1 = 0.1$, $\mu_1 = 0.3$, $\lambda_2 = 0.08$, $\mu_2 = 0.3$, $\theta_2 = 0$; square: $\lambda_1 = 0.1$, $\mu_1 = 0.3$, $\lambda_2 = 0.08$, $\mu_2 = 0.3$, $\theta_2 = 0.1$.

interlayer recovery mechanism plays a critical role in the increase of stiflers if the interlayer contagion rate is small, while the contagion mechanism between layers dominates the enhancing effect if the interlayer contagion rate becomes large. This is because a large θ_1 can significantly increase the

fraction of spreaders in each evolution step. In contrast, θ_2 only has influence on individuals who are stiflers in one layer but nonstiflers in the other layer, which does not increase the fraction of spreaders in both layers.

In Figs. 11(a)–11(c), we present effects of interlayer recovery process on the stationary fraction of stiflers. We change diffusion parameters within each layer and set $\theta_1 = 0$ in Fig. 11(a) while fix λ_1, μ_1, λ_2, μ_2, and vary θ_1 in Fig. 11(b) to see the influence of θ_2 under different circumstances. The fraction of stiflers still shows the trend of a sharp increase followed immediately by a slow decline. Additionally, in Fig. 11(c), we change λ_2 to control diffusion results within layer 2 and fix λ_1, μ_1, θ_1 to observe how changes on layer 2 affect the enhancing effect characterized by θ_2 on layer 1. Simulations show that the promoting effect of interlayer recovery process on layer 1 is strengthened when information spreads more sufficiently in layer 2. It can also be observed that under all circumstances a small interlayer recovery rate has a maximal effect on promoting information diffusion. Moreover, all peak points appear in the vicinity of $\theta_2 = 0.006 \sim 0.01$ in our simulations.

Up to now, all simulations are implemented in uncorrelated multiplex networks. However, there is no denying the fact that degree correlations do exist in realistic social networks, i.e., hubs are likely to be hubs in all platforms. Therefore, we further investigate how interlayer recovery process affects information diffusion in maximally positive correlated scale-free multiplex networks for comparison, see simulation results in Figs. 11(d)–11(f). In this maximally positive correlated case,
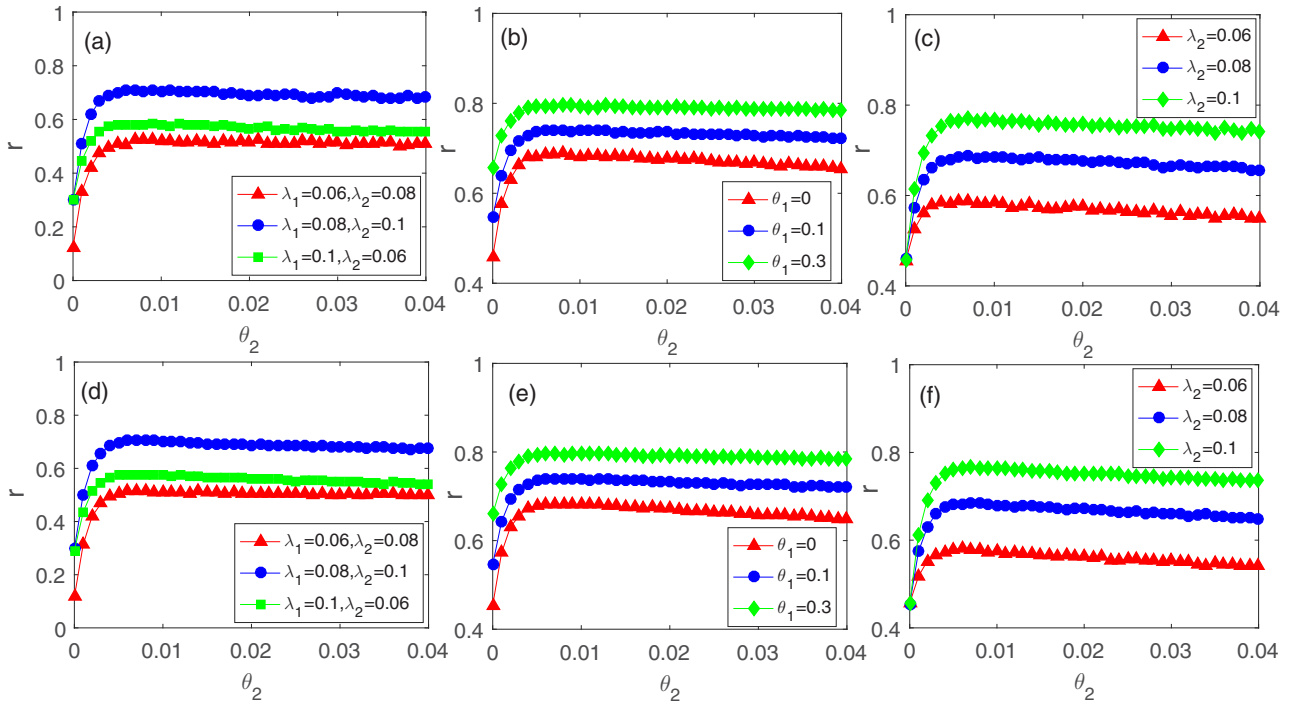

FIG. 11. Effects of the interlayer recovery process on the stationary fraction of stiflers in the two layer scale-free multiplex networks. (a)–(c) show different situations in uncorrelated multiplex networks while (d)–(f) give corresponding results in maximally positive correlated networks. (a), (d): $\theta_1 = 0$, $\mu_1 = \mu_2 = 0.3$ are fixed for all curves and the other parameters are set as follows: triangle: $\lambda_1 = 0.06$, $\lambda_2 = 0.08$; circle: $\lambda_1 = 0.08$, $\lambda_2 = 0.1$; square: $\lambda_1 = 0.1$, $\lambda_2 = 0.06$. (b), (e): We set $\theta_1 = 0, 0.1$ and 0.3 respectively and other parameters are fixed as: $\lambda_1 = 0.1$, $\mu_1 = 0.3$, $\lambda_2 = 0.08$, $\mu_2 = 0.3$. (c), (f): We set $\theta_1 = 0$, $\lambda_1 = 0.1$, $\mu_1 = 0.3$, $\mu_2 = 0.3$ and change λ_2 as 0.06, 0.08 and 0.1, respectively.

the nodes degrees in different layers are maximally correlated in their degree order [36]. Note that the degree distribution and the network structure in a single layer is unchanged. Results show that there is almost no difference between uncorrelated structure and maximally positive correlated structure in our model, except the curves in maximally positive correlated situations are smoother, which represent smaller fluctuations in different simulations. We give the following explanations. When information diffusion takes place in a single layer following our modified SIR model, hubs can easily receive rumors and become a spreader. Meanwhile, the recovery rate of the hub i $\mu^* = \mu_{j1} + (1 - \mu_{j1})[1 - (1 - \mu_{j2})^{k(i)r_j(t)}]$ is close to 1 even when $r_j(t)$ is relatively small, for the reason that $k(i)$, which represents the degree of hub i is quite large. In other words, hubs can quickly change status from spreaders to stiflers within a layer because of the contact-recovery mechanism in our model. The effects of interlayer recovery process for hubs is much smaller than that within a single layer and thus the degree correlations between layers make no difference on the final results.

V. CONCLUSIONS AND DISCUSSIONS

In this paper we propose a modified rumor-spreading SIR model, which incorporates an interlayer recovery mechanisms to describe information diffusion processes in online social networks. We examine how dynamical mechanisms between layers, especially interlayer recovery mechanism, affect the scope of information delivery in multiplex well-mixed population and ER-ER multiplex networks. A theoretical framework is presented by combining the homogeneous mean-field method and the Markov chain approach. Results show that both interlayer recovery and contagion mechanisms can promote information diffusion processes. The contagion mechanism between layers greatly promotes the fraction of stiflers in each layer, especially when the contagion rate is large and close to 1. As the interlayer recovery rate grows, the fraction of stiflers exhibits a sharp increase and then a slow decrease. This indicates a phenomenon that a small interlayer recovery transmission rate has a maximum effect on promoting information diffusion. Remarkably, the optimal interlayer

recovery rate that achieves the maximal enhancement can be predicted by solving the equations numerically. Moreover, the enhancing effect of the interlayer recovery mechanism on a certain layer can be strengthened if information spreads more sufficiently within the counterpart layer. We further apply our model to multiplex systems of two scale-free networks. Simulations show the same phenomenon as we observed in ER-ER multiplex networks. In addition, when dealing with how interlayer recovery process affects information diffusion, we find the degree correlations between layers make no difference.

Our work not only demonstrates a possible solution in designing efficient spreading strategies in multiplex online social networks, but also provides a theoretical framework to explain and predict information diffusions involving interlayer dynamics for future works. For instance, the simultaneous transmission of two pieces of competing information, the diffusion of controversial topics which contain different viewpoints. The interlayer recovery rate in this work can simply be substituted by the probability that an individual delivers the opposite information from one layer to the other. Furthermore, a more accurate mathematical description of interlayer dynamical processes, which can better illustrate the emergence of optimal interlayer recovery rate is also worthy studying in the future.

APPENDIX: ROBUSTNESS OF T_c

We supplement detailed studies of the robustness of T_c in this Appendix. We use the same ER-ER multiplex system where $N = 10^4$, $\langle k \rangle_1 = 20$, $\langle k \rangle_2 = 30$ as in Sec. IV B.

First, we present temporal dynamics of the fraction of stiflers on layer 1 under different circumstances in Fig. 12. Each point on the curves is the average of 100 simulations. Results show that the fraction of stiflers on each layer increases
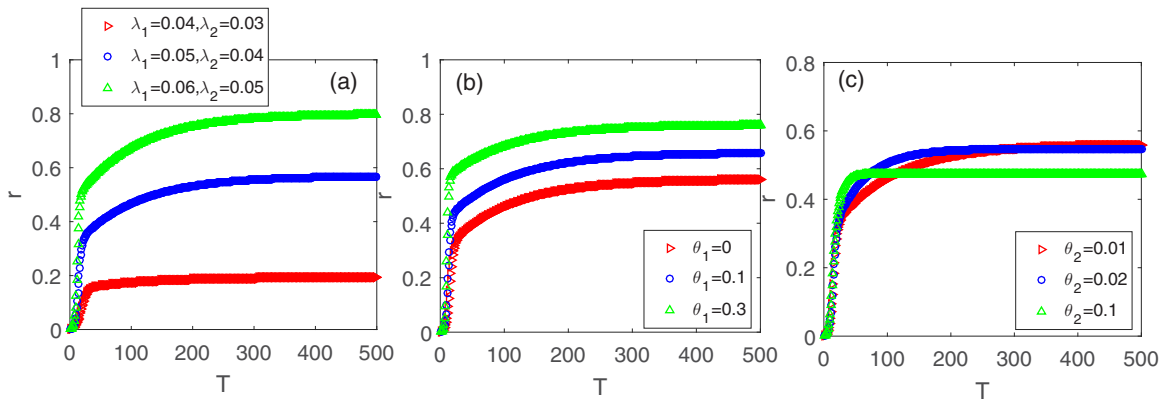

FIG. 12. Temporal dynamics of the fraction of stiflers on layer 1 under different circumstances. (a) $\mu_1 = 0.4, \mu_2 = 0.6, \theta_1 = 0, \theta_2 = 0.01$, other parameters: red line: $\lambda_1 = 0.04, \lambda_2 = 0.03$; blue line: $\lambda_1 = 0.05, \lambda_2 = 0.04$; green line: $\lambda_1 = 0.06, \lambda_2 = 0.05$. (b) We fix $\lambda_1 = 0.05, \mu_1 = 0.4, \lambda_2 = 0.04, \mu_2 = 0.6, \theta_2 = 0.01$ and change $\theta_1 = 0, 0.1, 0.3$, respectively. (c) We fix $\lambda_1 = 0.05, \mu_1 = 0.4, \lambda_2 = 0.04, \mu_2 = 0.6, \theta_1 = 0$ and let $\theta_2 = 0.01, 0.02, 0.1$, respectively.
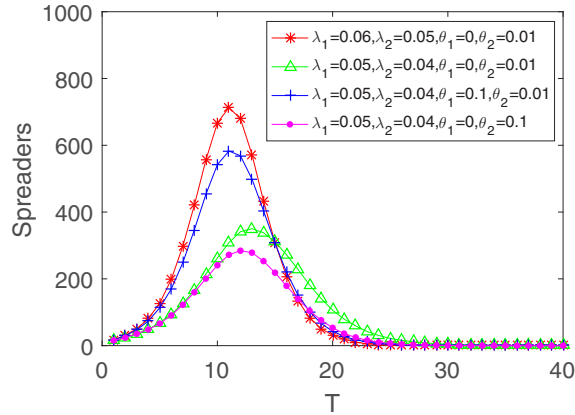
FIG. 13. Temporal dynamics of the fraction of spreaders on layer 1 in different parameter groups. $\mu_1 = 0.4, \mu_2 = 0.6$ are fixed. Other parameters are set as follows: red line: $\lambda_1 = 0.06, \lambda_2 = 0.05, \theta_1 = 0, \theta_2 = 0.01$; green line: $\lambda_1 = 0.05, \lambda_2 = 0.04, \theta_1 = 0, \theta_2 = 0.01$; blue line: $\lambda_1 = 0.05, \lambda_2 = 0.04, \theta_1 = 0.1, \theta_2 = 0.01$; magenta line: $\lambda_1 = 0.05, \lambda_2 = 0.04, \theta_1 = 0, \theta_2 = 0.1$.

rapidly in the first dozens of steps, then grows gradually each step, and finally reaches steady state. According to our definition in Sec. III, T_c first appears in the vicinity of $T = 30$ and can be considered sustained until about $T = 200$, if θ_2 is quite small. It can be concluded from Figs. 12(a) and 12(b) that T_c mainly depends on the parameters λ_i and μ_i, which control the dynamical processes within each layer and θ_1 accelerates the diffusion process which makes T_c appears earlier. In addition, θ_2 significantly shortens the processes from slowly increasing state to the final steady state but have little effects on the first appearance time of T_c, as shown in Fig. 12(c).

Besides, in Fig. 13, we show temporal dynamics of the fraction of spreaders on layer 1 in different parameter groups as a verification. Simulations show that under all circumstances, T_c first appears at about $T = 30$.

In conclusion, T_c is relatively robust because it is almost unaffected by the interlayer dynamical processes. Moreover, it is mainly determined by λ_i and μ_i. Thus T_c can be estimated empirically, as we have implemented in Sec. IV B.

[1] O. Yăgan, D. Qian, J. Zhang, and D. Cochran, IEEE J. Sel. Areas Commun. **31**, 1038 (2013).

[2] C. Granell, S. Gomez, and A. Arenas, Phys. Rev. E **90**, 012808 (2014).

[3] S. Pei, L. Muchnik, J. S. Andrade, Jr., Z. Zheng, and H. A. Makse, Sci. Rep. **4**, 5547 (2014).

[4] L. Weng, F. Menczer, and Y.-Y. Ahn, Sci. Rep. **3**, 2522 (2013).

[5] S. Pei and H. A. Makse, J. Stat. Mech.: Theor. Exp. (2013) P12002.

[6] M. DeDomenico, A. Sole-Ribalta, E. Cozzo, M. Kivela, Y. Moreno, M. A. Porter, S. Gomez, and A. Arenas, Phys. Rev. X **3**, 041022 (2013).

[7] S. Gomez, A. Diaz-Guilera, J. Gomez-Gardenes, C. J. Perez-Vicente, Y. Moreno, and A. Arenas, Phys. Rev. Lett. **110**, 028701 (2013).

[8] S. Boccaletti, G. Bianconi, R. Criado, C. I. del Genio, J. Gomez-Gardenes, M. Romance, I. Sendina-Nadal, Z. Wang, and M. Zanin, Phys. Rep. **544**, 1 (2014).

[9] J. Gómez-Gardenes, I. Reinares, A. Arenas, and L. M. Floria, Sci. Rep. **2**, 620 (2012).

[10] O. Yăgan and V. Gligor, Phys. Rev. E **86**, 036103 (2012).

[11] X. Teng, S. Pei, F. Morone, and H. A. Makse, Sci. Rep. **6**, 36043 (2016).

[12] W. Li, S. Tang, W. Fang, Q. Guo, X. Zhang, and Z. Zheng, Phys. Rev. E **92**, 042810 (2015).

[13] M. Kivelä, A. Arenas, M. Barthelemy, J. P. Gleeson, Y. Moreno, and M. A. Porter, J. Complex Netw. **2**, 203 (2014).

[14] G. Menichetti, D. Remondini, P. Panzarasa, R. J. Mondragn, and G. Bianconi, PLoS ONE **9**, e97857 (2014).

[15] Q. Guo, X. Jiang, Y. Lei, M. Li, Y. Ma, and Z. Zheng, Phys. Rev. E **91**, 012822 (2015).

[16] P. J. Mucha, T. Richardson, K. Macon, M. A. Porter, and J.-P. Onnela, Science **328**, 876 (2010).

[17] V. Nicosia and V. Latora, Phys. Rev. E **92**, 032805 (2015).

[18] Y. Hu, S. Havlin, and H. A. Makse, Phys. Rev. X **4**, 021031 (2014).

[19] F. Radicchi and G. Bianconi, Phys. Rev. X **7**, 011013 (2017).

[20] J. Sanz, C.-Y. Xia, S. Meloni, and Y. Moreno, Phys. Rev. X **4**, 041005 (2014).

[21] F. Darabi Sahneh and C. Scoglio, Phys. Rev. E **89**, 062817 (2014).

[22] V. Marceau, P.-A. Noël, L. Hébert-Dufresne, A. Allard, and L. J. Dubé, Phys. Rev. E **84**, 026105 (2011).

[23] S. Funk and V. A. A. Jansen, Phys. Rev. E **81**, 036118 (2010).

[24] A. Saumell-Mendiola, M. Á. Serrano, and M. Boguñá, Phys. Rev. E **86**, 026106 (2012).

[25] J. M. Epstein, J. Parker, D. Cummings, and R. A. Hammond, PLoS ONE **3**, e3955 (2008).

[26] L. D. Valdez, P. A. Macri, H. E. Stanley, and L. A. Braunstein, Phys. Rev. E **88**, 050803(R) (2013).

[27] M. Dickison, S. Havlin, and H. E. Stanley, Phys. Rev. E **85**, 066109 (2012).

[28] C. Buono, L. G. Alvarez-Zuzek, P. A. Macri, and L. A. Braunstein, PloS ONE **9**, e92200 (2014).

[29] C. Granell, S. Gómez, and A. Arenas, Phys. Rev. Lett. **111**, 128701 (2013).

[30] S. Yan, S. Tang, S. Pei, S. Jiang, X. Zhang, W. Ding, and Z. Zheng, Physica A (Amsterdam) **392**, 3846 (2013).

[31] R. Parshani, S. V. Buldyrev, and S. Havlin, Phys. Rev. Lett. **105**, 048701 (2010).

[32] J. Gao, S. V. Buldyrev, H. E. Stanley, and S. Havlin, Nature Phys. **8**, 40 (2012).

[33] S. V. Buldyrev, R. Parshani, G. Paul, H. E. Stanley, and S. Havlin, Nature (London) **464**, 1025 (2010).

[34] E. Cozzo, R. A. Bãnos, S. Meloni, and Y. Moreno, Phys. Rev. E **88**, 050801(R) (2013).

[35] D. J. Daley and D. G. Kendall, Nature (London) **204**, 1118 (1964).

[36] B. Min, S. D. Yi, K. M. Lee, and K. I. Goh, Phys. Rev. E **89**, 042811 (2014).

[37] A. Barrat, M. Barthélemy, and A. Vespignani, *Dynamical Processes on Complex Networks*, 1st ed. (Cambridge University Press, Cambridge, 2008).

[38] W. Wood, Ann. Rev. Psych. **51**, 539 (2000).

[39] Z. K. Zhang, C. Liu, X. X. Zhan, X. Lu, C. X. Zhang, and Y. C. Zhang, Phys. Rep. **651**, 1 (2016).

[40] S. A. Myers, C.-G. Zhu, and J. Leskovec, Information diffusion and external influence in networks, in *Proceedings of the 18th ACM SIGKDD International Conference on Knowledge Discovery and Data Mining* (ACM Press, New York, 2012), pp. 33–41.

[41] D. H. Zanette, Phys. Rev. E **65**, 041908 (2002).

[42] D. H. Zanette and S. Gil, Physica D (Amsterdam) **224**, 156 (2006).

[43] M. E. J. Newman, Phys. Rev. E **66**, 016128 (2002).

[44] M. Á. Serrano and M. Boguñá, Phys. Rev. Lett. **97**, 088701 (2006).

[45] Z. Wu, C. Lagorio, L. A. Braunstein, R. Cohen, S. Havlin, and H. E. Stanley, Phys. Rev. E **75**, 066110 (2007).

[46] M. E. J. Newman, S. H. Strogatz, and D. J. Watts, Phys. Rev. E **64**, 026118 (2001).

[47] M. Á. Serrano, D. Krioukov, and M. Boguñá, Phys. Rev. Lett. **106**, 048701 (2011).

[48] A. Allard, L. Hébert-Dufresne, P.-A. Noël, V. Marceau, and L. J. Dubé, J. Phys. A **45**, 405005 (2012).

[49] J. I. Venn, Philos. Mag. **10**, 1 (1880).

[50] A.-L. Barabási and R. Albert, Science **286**, 509 (1999).